

# Derivatization of Free Radicals in an Isopropanol Plasma Polymer Film: The First Step toward Polymer Grafting

S. Ershov,<sup>†</sup> F. Khelifa,<sup>‡</sup> P. Dubois,<sup>‡,§</sup> and R. Snyders<sup>\*,†,§</sup>

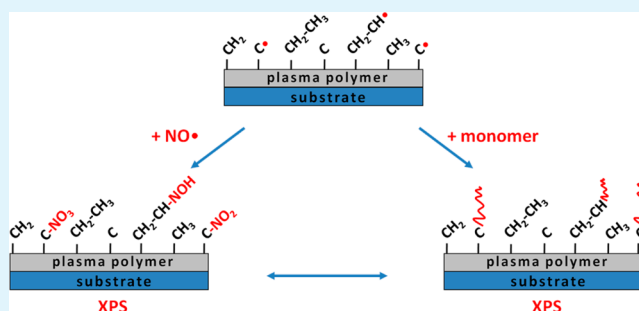
<sup>†</sup>Chimie des Interactions Plasma Surfaces, Center of Innovation and Research in Materials and Polymers (CIRMAP), <sup>‡</sup>Laboratory of Polymeric and Composite Materials, Center of Innovation and Research in Materials and Polymers (CIRMAP), University of Mons UMONS, Place du Parc 23, 7000 Mons, Belgium

<sup>§</sup>Materia Nova Research Center, Parc Initialis, Avenue N. Copernic 1, 7000 Mons, Belgium

**ABSTRACT:** Plasma-polymerized films (PPF) synthesized by plasma-enhanced chemical vapor deposition (PECVD) find increasing applications in biomedicine and differ in many ways from conventional polymers. One of the most specific properties of the PPF is the high reactivity of its free-radical-rich surface, arising from the deposition mechanism. Although generally considered as a disadvantage leading to the aging of the PPF, reactivity of the plasma-treated polymers and PPF surfaces can be beneficially employed, for example, for grafting of a specific chemical functionality or short polymer chains.

The quantitative evaluation of the surface radical density of the PPF is thus considered as the necessary preparatory step toward any subsequent grafting reaction. In the present study, the surface radical density of an isopropanol-based PPF was quantitatively determined by a combination of NO chemical derivatization and X-ray photoelectron spectroscopy (XPS). Once the derivatization conditions were optimized, the radical density, derived from at % N determined by XPS, was evaluated as a function of the deposition power. It was found out that the surface density of free radicals presents a maximum for the deposition power of 200 W ( $\sim 2.3 \times 10^{14}$  spin/cm<sup>2</sup>) and it stabilizes ( $\sim 2.1 \times 10^{14}$  spin/cm<sup>2</sup>) with further power increase. XPS findings were supported by in situ FTIR measurements that provided additional information about the degree of plasma fragmentation denoting fragmentation saturation for a deposition power of 200 W. By fitting the N1s peak it was possible to identify primary, secondary and tertiary radicals and to study their respective evolutions with different deposition conditions. Angle-resolved XPS analysis allowed the in-depth distribution of radicals to be addressed, revealing that on the top surface, primary, and secondary radicals are dominating, whereas more tertiary radicals are present in the subsurface region. Finally, some preliminary chemical grafting experiments have allowed the relevance of derivatization results to be cross-checked.

**KEYWORDS:** plasma polymerization, surface free-radical density, chemical derivatization, polymer grafting



## 1. INTRODUCTION

Plasma-polymerized films (PPF) used for example in biomedical applications<sup>1–5</sup> and microelectronic devices<sup>6,7</sup> differ in many ways from conventional polymers and offer several appealing advantages. They can be easily deposited in a range of thicknesses from several hundreds of nanometers to more than one micrometer. They normally exhibit a highly branched and cross-linked structure free of pinholes. Good adhesion to different substrates, such as conventional polymers, glasses and metals, is another notable feature. Careful control of the deposition parameters allows the chemical and physical properties of the PPF to be varied and tailored in order to best comply with the intended application.<sup>8–10</sup>

PPF are usually synthesized by plasma-enhanced chemical vapor deposition (PECVD), which is based on supplying electrical energy to an organic precursor in the gaseous phase. Thus a plasma is created where numerous electron impact-based bond scissions of the precursor molecules are accompanied by free-radical formation of the coating.<sup>11–13</sup>

Plasma-induced and plasma-state polymerization, competitive counterproductive ablation, as well as VUV radiation lead to the synthesis of the highly cross-linked film, characterized by a network of irregular nonrepetitive polymer structures.<sup>9,14</sup> Numerous species present in the plasma (electrons, atoms, excited molecules and fragments, radicals, ions, etc.) react with each other and with the growing film via a multitude of interaction pathways. This often leads to the unspecific functionalization of the highly reactive surface of the PPF, which differs greatly from the surface of conventional polymers.<sup>15</sup> One of the most specific properties of the PPF is that both its surface and subsurface regions are rich in free radicals arising from the gas phase during fragmentation and generated on the growing surface through interaction with plasma particles and VUV radiation.<sup>16,17</sup> Radicals possess an

Received: January 30, 2013

Accepted: April 22, 2013

Published: April 22, 2013

unpaired electron in their structure and exhibit a huge potential to react once removed from the deposition chamber and exposed to an ambient or specific environment. In the air radicals would undergo manifold reactions with omnipresent oxygen resulting in the incorporation of various oxygen-containing groups. This process of uncontrollable and, in most cases, undesirable modification of the surface chemistry is commonly referred to as the aging of the PPF.<sup>18–20</sup> So although generally considered as a disadvantage, reactivity of the plasma treated polymer and PPF surfaces can turn out to be advantageous when exploited carefully, for example for grafting of a specific chemical functionality or covalent immobilization of biomolecules.<sup>21–26</sup> In this case, free radicals may serve as a robust designing tool for surface technology.

Evaluation of the density of surface free radicals is an important prerequisite in order to understand grafting or functionalization mechanisms of the PPF. Indeed, a low density of surface free radicals might lead to an insufficient coverage of the surface by the covalently bound molecules, whereas too high density may result in numerous termination reactions and loss of reactivity.<sup>27,28</sup>

A number of studies have already been dedicated to the identification and quantification of free-radical species on the surface of PPF or plasma treated polymers by different physical and chemical techniques.<sup>29–34</sup> Electron spin resonance (ESR) offers the advantage of high sensitivity but requires a large surface-to-volume ratio making the analysis of a single thin film difficult. Chemical labeling (and subsequent XPS analysis) of surface free radicals can be carried out either with gaseous or liquid derivatizing agents. Among others NO is a very reactive radical gas, which allows various types of carbon-centered radicals to be distinguished through corresponding binding energy shifts of derivatization products in an XPS spectra. Labeling with selective iodine gas yields a lower surface radical concentration than with NO,<sup>16</sup> but has the advantage that its reaction products are easier to detect with XPS. Wet chemical derivatization methods (accompanied by absorption spectroscopy) confront the challenges of the oxygen-free transfer (for 2,2-diphenyl-1-picrylhydrazyl (DPPH)), necessity to derivatize postoxidation products (for iodide), unknown analysis depth and side reactions of labeling agents with various functional groups also present at the surface (for both). However, absolute quantification of the radical density in all labeling techniques is not straightforward because of the absence of calibration methods and the numerous assumptions (such as density of the film in the surface regions, reaction volume, etc.) that must be taken into account during the data analysis.<sup>16,35,36</sup> Among other methods available for the detection of free radicals trapped within polymer materials fluorescence labeling should also be mentioned.<sup>37</sup>

In the present work, the quantitative evaluation of the surface radical density has been performed on an isopropanol-based PPF. Such an evaluation is considered to be a necessary preparatory step before subsequent polymer grafting via a free-radical polymerization reaction, which is initiated directly from the isopropanol-based PPF. NO has been selected as the labeling agent because of its fast and efficient reactive capacity and the possibility of distinguishing between different derivatization products (and hence C-centered radical types) in XPS spectra. First, the method of chemical derivatization with NO was validated for the specific set of chambers and experimental conditions used in this study. Once the derivatization conditions were optimized, the radical density

was evaluated as a function of deposition power. In situ Fourier transform infrared spectroscopy (FTIR) measurements provided extra information about the degree of plasma fragmentation. Angle-resolved XPS data helped to draw some conclusions about the in-depth distribution of free radicals. Finally, preliminary grafting experiments via free-radical polymerization reactions allowed the relevance of the derivatization results to be cross-checked.

## 2. EXPERIMENTAL SECTION

PPF were synthesized on p-type (B-doped) Si substrates (acetone/methanol precleaned) with isopropanol (MERCK, 99.8%) gas in a lab-scale deposition chamber. Isopropanol was selected as a saturated hydrocarbon containing oxygen in order to allow better differentiation in XPS spectra between the PPF and the grafted layer. The distance between the inductive coil, powered by a CESAR 1310 Generator from Advanced Energy, and the substrate was fixed at 5.5 cm. Evacuating the chamber by a combination of scroll and turbomolecular pumps allowed the base pressure in the order of  $1 \times 10^{-4}$  Pa to be obtained, whereas the working pressure of 6.67 Pa was kept constant by a throttle valve. The amounts of gases (isopropanol, Ar, O<sub>2</sub>) in the gas mixture were controlled independently by separate mass flow controllers. Prior to deposition, substrates were treated for 10 min in an Ar–O<sub>2</sub> discharge (25 sccm each) at a working pressure of 6.67 Pa and an injected RF power ( $P_{RF}$ ) of 100 W in order to get rid of the atmospheric surface pollution. PPF depositions with 5 sccm of isopropanol were carried out mainly (if not stated otherwise) for 5 min at  $P_{RF} = 200$  W for the derivatization technique evaluation giving rise to a thickness of  $850 \pm 42.5$  nm as measured by a mechanical profilometer Dektak 150 from Veeco. In the second part of the work,  $P_{RF}$  was varied from 65 to 400 W.

Immediately after deposition, PPF samples were transferred into a separate vacuum chamber (base pressure  $<1 \times 10^{-3}$  Pa) for derivatization tests without exposure to the ambient atmosphere. The transfer under vacuum (pressure around  $1 \times 10^{-4}$  Pa) took  $\sim 3$  min if not stated otherwise. The labeling agent, nitric oxide (Air Liquide, 99.9%), was introduced into the chamber until the desired pressure (Pirani gauge controlled) was attained under static conditions (turbo pump blocked using a gate valve).

Grafting experiments with 2-ethylhexyl acrylate (EHA, VWR, 99%) were performed in the same vacuum chamber as the derivatization tests. Prior to grafting, EHA was passed through a basic alumina column to remove the stabilizing agent. Introduction of the liquid monomer into the chamber took place through the valve located above the substrate-holder. In order to avoid violent spraying of EHA upon contact with the base vacuum of the chamber and to ensure complete coverage of the PPF sample by the monomer, the pressure was increased with Ar to slightly below atmospheric pressure before the actual polymerization test began. During the test the chamber was heated up to 50 °C by an external heater to guarantee an efficient polymerization reaction. Grafting experiments lasted 60 min, the empirically estimated optimum time for sufficient grafting. After the grafting experiments, samples were washed twice with chloroform (Alfa Aesar, 99+ %) for 5 min so that physisorbed (monomer/polymer) layers were removed and only covalently bound poly(EHA) polymer chains remained on the PPF surface.

The set of PECVD and derivatization/grafting chambers is presented in Figure 1.

Chemical composition of the PPF was evaluated by X-ray photoelectron spectroscopy (XPS) on a VERSAPROBE PHI 5000 hemispherical analyzer from Physical Electronics with a base pressure of  $<3 \times 10^{-7}$  Pa. The X-ray photoelectron spectra were collected mainly (if not stated otherwise) at the takeoff angle of 45° with respect to the electron energy analyzer, operating in constant analyzer energy (CAE) mode (23.50 eV). The spectra were recorded with the monochromatic Al K<sub>α</sub> radiation (15 kV, 25 W) with a highly focused beam size of 100 μm. The energy resolution was 0.7 eV. The binding energy scale of the spectra was calibrated with respect to the aliphatic component of the C1s peak at 285 eV.<sup>38,39</sup> Eventual surface charging

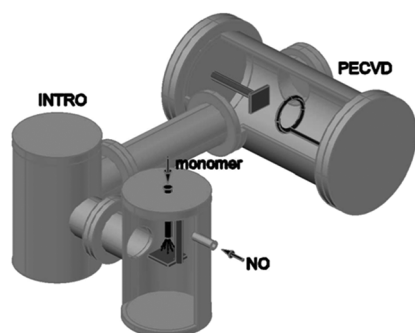


**Figure 1.** Schematic drawing of PECVD and derivatization/grafting chambers.

was compensated by a built-in electron gun and an argon ion neutralizer. N 1s spectra were recorded with a high pass energy (58.70 eV) in order to reduce the acquisition time and to avoid degradation of some NO<sub>x</sub> compounds but at the same time to obtain a good signal-to-noise ratio, which is essential for the data analysis of very small amounts of nitrogen.

Diagnostic of the isopropanol plasma by using in situ FTIR spectroscopy was performed on an Agilent 670 FT-IR spectrometer aligned with a multireflection mirror system. Thirteen mirrors, resulting in an optical path length of the 26 m, allow a sufficient signal-to-noise ratio to be accumulated, because of the beam's multiple passes through the discharge. Spectra from 600 to 4000 cm<sup>-1</sup> were taken with a resolution of 4 cm<sup>-1</sup> and 50 scans. For data treatment the Blackman Harris 4 Term apodization function was applied.

### 3. RESULTS

**3.1. Validation of the Method.** Adaptation of the derivatization method for the present experimental conditions was mainly an extension of the work performed by Wilken et al.,<sup>27,31</sup> which was focused on the search of optimal parameters for chemical labeling of surface free radicals with NO gas. NO pressure during derivatization, NO treatment time, transfer time between PECVD and derivatization chambers as well as the aging of the derivatized film under air, associated with the transfer time to the XPS chamber, have been performed on the PPF deposited in pure isopropanol plasma at 200 W for 5 min treatment performed at 200 W in pure isopropanol plasma. In pursuit of optimal conditions for efficient derivatization first the NO pressure and NO treatment time have been varied. Graphs displaying nitrogen content (at % N) in the films determined by XPS as a function of those parameters are presented in Figure 2.

Figure 2a shows that at % N, and therefore the density of derivatized free radicals, grows with the increase in NO pressure from 10 to 100 mbar (due to the increasing reservoir of NO molecules for the labeling reaction) then remains relatively stable up to 500 mbar. This almost flat plateau means that already at 100 mbar, after 15 min reaction time, there is enough NO supplied to trap all the accessible radicals. Therefore, for the actual derivatization experiments the NO pressure of 100 mbar has been selected. Figure 2b shows that at % N does not depend on the NO treatment time, which is consistent with the high reactivity of nitric oxide toward carbon-centered radicals.<sup>16,27</sup> A treatment time of 15 min has therefore been chosen. The NO treatment time (15 min) as well as the NO pressure (100 mbar) chosen for the present study are in good agreement with the values reported by Wilken et al. for their derivatization experiments of VUV irradiated PE, PP, and PS surfaces.<sup>27</sup>

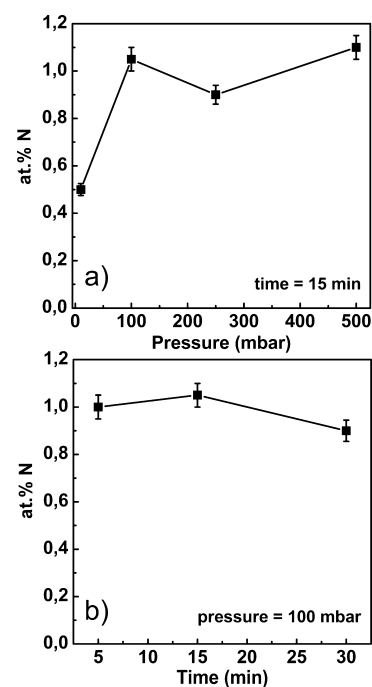
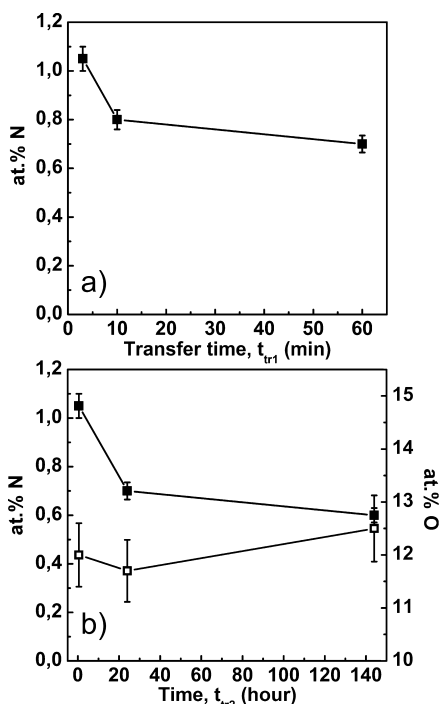


**Figure 2.** XPS-determined at % N on the surface of the PPF synthesized with  $P_{RF} = 200$  W as a function of (a) NO pressure and (b) NO treatment time.

Other parameters more specifically related to this process have also been evaluated. The transfer time of the PPF from the deposition to the derivatization chamber under vacuum ( $t_{tr1}$ ) is associated with the lifetime of radicals under vacuum, while the transfer time of derivatized samples in the air from the derivatization chamber to the XPS chamber ( $t_{tr2}$ ) is important for the reliability of the chemical analysis. The effect of these parameters needs to be carefully evaluated in order to draw accurate conclusions from the measurements.

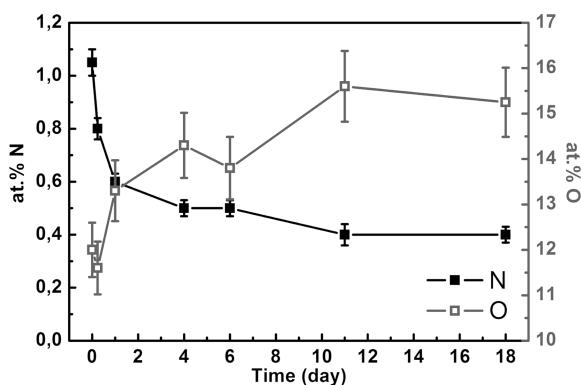
Figure 3a displays the evolution of at % N as a function of  $t_{tr1}$ . A decrease of the nitrogen content from  $\sim 1.05$  to  $\sim 0.80$  at % in the first ten minutes of residing in vacuum is followed by a much smaller decrease to 0.7 at % during the next 60 min. The rather rapid initial decrease of nitrogen may be attributed either to termination/recombination reactions of some radicals or to nonideal vacuum conditions in the system. Indeed, a base pressure of  $1 \times 10^{-4}$  Pa allows the presence of a few reactive oxygen-based species ( $O_2$ ,  $H_2O$ ), which are capable of trapping surface free radicals. To keep the maximum amount of reactive radicals alive on the surface of the PPF before chemical labeling with NO, we have chosen the empirically determined transfer time of  $\sim 3$  min for derivatization tests.

Figure 3b shows that at % N continuously decreases with  $t_{tr2}$ , whereas the oxygen content remains relatively stable. This decrease of nitrogen is supposedly attributed to the surface adaptation of the PPF, namely reorganization of the film surface because of the interfacial energy differences upon contact with the air, and/or to accumulating surface contamination from atmospheric pollution.<sup>28</sup> To limit these phenomena before XPS analysis, we set the minimal transfer time between chambers with inevitable exposure to the air to 15 min for all derivatization tests. These tests have shown how complicated and step-dependent is the derivatization of free radicals present on the PPF samples. Therefore, a rigorous methodology needs to be defined in order to allow reliable comprehension of data.



**Figure 3.** XPS-determined PPF ( $P_{RF} = 200$  W) surface content of at % N as a function of (a) transfer time,  $t_{tr1}$ , between deposition and derivatization chambers under vacuum and (b) at % N (in full black squares) and at % O (in white squares) as a function of atmosphere exposure time,  $t_{tr2}$ , of derivatized samples prior to XPS analysis.

**3.2. Surface Free-Radical Study.** An aging test of the PPF under the ambient atmosphere has been carried out prior to the actual derivatization study. Alterations of at % N and oxygen content (at % O) of the PPF, exposed to the air for different time intervals prior to derivatization, are displayed in Figure 4.



**Figure 4.** XPS-determined at % N and at % O on the surface of the PPF synthesized at  $P_{RF} = 200$  W as a function of the atmosphere exposure time prior to the derivatization.

It can be seen that the decrease of at % N occurs in parallel with an increase of at % O as the time between the deposition of the PPF and its subsequent derivatization increases. The uptake of oxygen is expected and is associated with the aging of the PPF driven by an autoxidation mechanism that exploits free radicals on the surface of the PPF for reactions with oxygen from the air.<sup>16,40,41</sup> During exposure to the air carbon-centered radicals on the surface react instantly with oxygen molecules. This rapid reaction leads to the formation of peroxy radicals,

the first product of the autoxidation process described in detail elsewhere.<sup>16,40,41</sup> In the course of autoxidation, metastable hydroperoxides slowly decay to form a large variety of more stable oxygen-containing products on the surface of the PPF. Thus, each radical can incorporate several oxygen atoms depending on the time of exposure that determines the reaction step of the autoxidation mechanism. It has been demonstrated that different oxygen-containing functional groups formed upon exposure to the air can undergo reactions with NO during the subsequent derivatization.<sup>16</sup> Therefore, it is impossible to differentiate in XPS spectra reaction products of surviving radicals with NO from reaction products of oxygen compounds with NO. Fast and then gradual decrease in at % N and increase in at % O with time can be attributed to the fact that increasingly oxygen-rich surface compounds can react differently with NO because of the nonlinear time scale of autoxidation. The limit of 0.4 at % N with the longest exposure time can be associated with NO reacting exclusively with various oxygen-containing groups formed on radicals in the course of rapidly beginning autoxidation.<sup>16,42</sup> Besides that, an air pressure of 10 times higher than NO derivatization pressure and the surface adaptation may also contribute to the changing character of the chemical composition.<sup>28</sup>

It is well-known and described that the power injected in the plasma ( $P_{RF}$ ) for a given precursor flow plays a major role in tuning the plasma chemistry and film structure in PECVD, including free-radical generation. Depending on the degree of precursor fragmentation, the strength of ion bombardment of the growing film, as well as the intensity of UV radiation from the plasma may vary considerably. Alterations of these parameters affect the structure of the growing PPF and especially the growing surface and subsurface front, where most of the free radicals are generated via bonds scissions through UV absorption or interaction with bombarding particles. The dependence of the surface density of free radicals on  $P_{RF}$  during the deposition of the PPF is presented in Figure 5.

The surface density of free radicals was deduced from the at % N determined by XPS according to the following eq 1

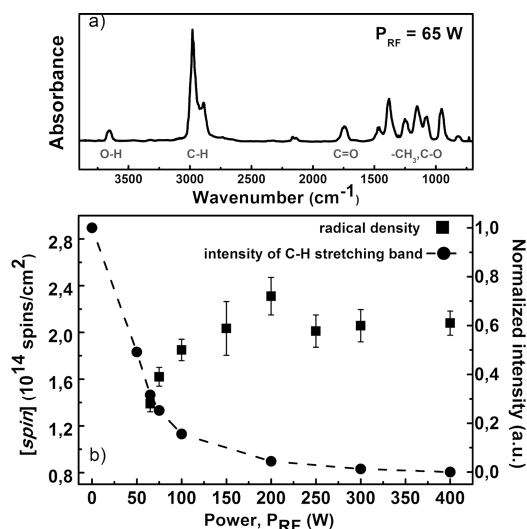


**Figure 5.** (a) In situ FTIR spectrum of the isopropanol plasma with  $P_{RF} = 65$  W and (b) the surface density of free radicals as well as the intensity of a C-H stretching band as a function of the deposition power.

$$[\text{spin}] = \text{at \% N} N_A \frac{M}{\rho} l \quad (1)$$

where at % N is the concentration of nitrogen in at %;  $N_A$  the Avogadro constant in  $\text{mol}^{-1}$ ;  $M$ , the molar mass of nitrogen in  $\text{g/mol}$ ;  $\rho$  – the density of the PPF in  $\text{g/cm}^3$ ; and  $l$ , the XPS analysis depth in cm. This calculation was carried out assuming the plasma polymer density of  $0.9 \text{ g/cm}^3$ ,<sup>27,31</sup> unchangeable radical concentration throughout the analysis depth of XPS of 5.9 nm and the fact that the majority of N-containing compounds originate from reactions of NO with C-centered radicals. Keeping in mind the possibility of reactions of NO with O-containing groups<sup>16</sup> but also taking into account the low amount of oxygen in the PPF ( $\sim 90$  at % C against  $\sim 10$  at % O), the last assumption seems relevant and might only lead to a minor overestimation of the density of C-centered radicals.

Figure 5b shows that the evolution of the surface density of free radicals with  $P_{\text{RF}}$  presents a maximum for  $P_{\text{RF}} = 200 \text{ W}$  ( $\sim 2.3 \times 10^{14} \text{ spin/cm}^2$ ) and then stabilizes for  $P_{\text{RF}} > 250 \text{ W}$  ( $\sim 2.1 \times 10^{14} \text{ spin/cm}^2$ ). The initial increase is consistent with the continuously increasing precursor fragmentation, particle bombardment and UV radiation which all give rise to a bigger number of surface free radicals. Then, the slight decrease supposedly originates from recombination reactions between radicals due to a too high radical density.<sup>27,28</sup> Assuming the average atom density of  $10^{15} \text{ at/cm}^2$  and the fact that in the cross-linked PPF most bonds are present as variations of carbon–carbon bonds, the mean distance between derivatized radicals is estimated to be in the order of half a nm (for the sample deposited with  $P_{\text{RF}} = 200 \text{ W}$ ). Deposition powers of  $P_{\text{RF}} = 300$  and  $400 \text{ W}$  presumably give rise to a higher number of radicals with the spacing smaller than the distance between the derivatized radicals. In this case closely located radicals might undergo recombination and thus decrease the overall radical density.

The precursor fragmentation has been evaluated by an in situ FTIR diagnostic. Figure 5a shows, as an example, an FTIR spectrum of the isopropanol plasma with  $P_{\text{RF}} = 65 \text{ W}$ . Several vibration bands attributed to different bonds within the isopropanol molecule (O–H, C–H,  $\text{CH}_3$ , C–O) as well as a newly formed C=O stretch band compose the spectrum of the fragmented isopropanol gas. Results of the in situ FTIR investigation of the plasma discharge as a function of  $P_{\text{RF}}$ , namely the changes in the intensity of the  $\text{CH}_3$  asymmetric stretch band ( $2977 \text{ cm}^{-1}$ ), are shown in Figure 5b. In comparison with the pure precursor (0 W in Figure 5b) the  $\text{CH}_3$  stretch band exhibits a decrease of 50% in its intensity for  $P_{\text{RF}} = 50 \text{ W}$  as the fragmentation events start to take place. The signal from all bands shows a dramatic decrease of 80% between 65 and 200 W. In this range the changes in degree of precursor fragmentation are the biggest as the continuously rising input power induces more efficient and abundant bond scissions. After 200 W changes in the degree of precursor fragmentation are considerably minimized once the fragmentation reaches its saturation because most of the intramolecular bonds have already been broken in the discharge at lower powers. In situ FTIR findings are in good agreement with the results of derivatization tests for varying power, correlating the gradual increase and the maximum surface radical concentration of  $\sim 2.3 \times 10^{14} \text{ spin/cm}^2$  in the range from 65 to 200 W with a continuously growing degree of plasma fragmentation in this range.

A deeper analysis of the radical chemistry can be obtained by deconvoluting the N1s spectrum of the derivatized surfaces. As an example, Figure 6 shows this deconvoluting for a PPF deposited at  $P_{\text{RF}} = 200 \text{ W}$ .

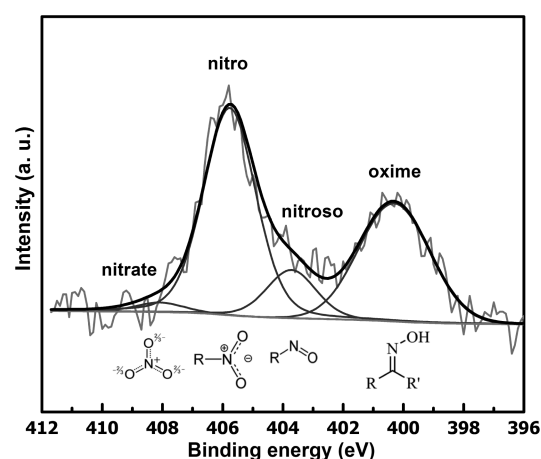


**Figure 6.** Fitted N 1s XPS peak for the derivatized PPF deposited with  $P_{\text{RF}} = 200 \text{ W}$ .

Four components, corresponding to various N-containing compounds, compose the spectrum. The types and binding energy positions of these compounds are presented in Table 1.

**Table 1.** The types and binding energy positions of N-containing compounds on the surface of the derivatized PPF

compd	formula	binding energy (eV)	ref
oxime	$\text{R}_1\text{R}_2\text{C}=\text{NOH}$	400.4	27,31
nitroso	$\text{R}-\text{N}=\text{O}$	403.7	27,31,42
nitro	$\text{RNO}_2$	405.8	27,31,42
nitrate	$\text{RONO}_2$	408.1	27,31,43

Reaction pathways in Figure 7 explain the origins of these compounds with respect to the type of carbon-centered radical

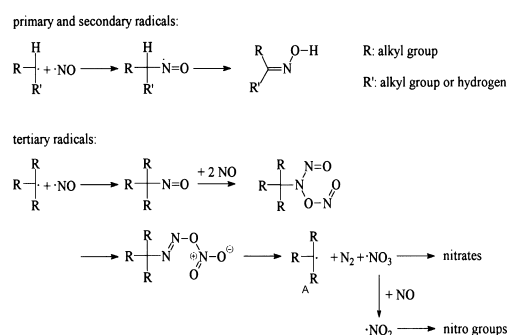


**Figure 7.** Reactions of formation of various N-containing compounds from free radicals.<sup>31</sup>

(primary, secondary or tertiary) being scavenged by nitric oxide.<sup>15,27,31</sup> The trapping of primary and secondary radicals by an NO molecule is accompanied by the hydrogen migration and consequent formation of oxime groups. In the case of tertiary radicals, once a nitroso group is formed via direct attachment, it can further react with NO into nitro and nitrate groups. Because of the fact that each of the mentioned chemical groups contain only one atom of nitrogen, oxime concentration

can be directly associated with the concentration of primary and secondary radicals, whereas the sum of nitroso, nitro, and nitrate groups can serve as a measure of tertiary radicals. The alterations in nitrogen content, deconvolved into four components, as a function of  $P_{RF}$  are shown in Figure 8.

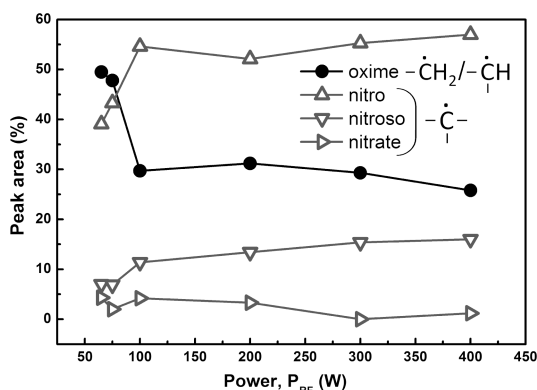


**Figure 8.** Relative concentration of various nitrogen-containing groups, derived from the deconvolution of corresponding N 1s XPS spectra, for different  $P_{RF}$ .

This figure shows that the oxime concentration decrease is accompanied by a comparable nitro concentration rise, whereas the values for nitroso and nitrate groups undergo only minor changes with increasing  $P_{RF}$ . These observations allow certain conclusions concerning the type of C-centered radicals to be drawn. At lower powers, the oxime groups are the most abundant (about 50% of the total amount of all groups), implying that there is the equal number of primary/secondary and tertiary radicals. However, for  $P_{RF} = 100$  W, the situation has already changed: the concentration of nitro groups has risen by  $\sim 15\%$ , and the concentration of oxime groups has fallen to  $\sim 30\%$ . At this power, fewer primary and secondary radicals are generated, whereas the amount of tertiary radicals increases. With further  $P_{RF}$  increase, the tendency of the gradual tertiary radical growth at the expense of primary and secondary radicals continues. Such a redistribution of radicals, from equally shared to dominating tertiary, can be associated with the rising energy input when increasing  $P_{RF}$ . In addition to the increasing fragmentation in the plasma phase and bombardment with plasma particles, stronger VUV radiation causes more efficient excitation of C–C, C–H, and C–O  $\sigma$  bonds in the growing film.

In view of the subsequent polymer grafting reaction, it is obvious that the distribution of radical types as a function of the PPF depth is also important. Results of nondestructive angle-resolved XPS analysis of the derivatized PPF surface providing this information without altering the film's chemistry are presented in Figure 9.

Changing the angle between the sample surface and the analyzer ( $15, 30, 45^\circ$ ) allows us to vary the sampling depth of the XPS analysis according to eq 2

$$d = 3\lambda \sin \Theta \quad (2)$$

where  $d$  is the sampling depth in nm;  $\lambda$ , the inelastic mean free path of an electron in nm; and  $\Theta$ , an angle between the sample surface and the analyzer. The data shows that the region close to the top surface region (up to 2.2 nm) contains more primary and secondary radicals than the deeper subsurface regions (up to 5.9 nm) where tertiary radicals prevail. The outermost PPF

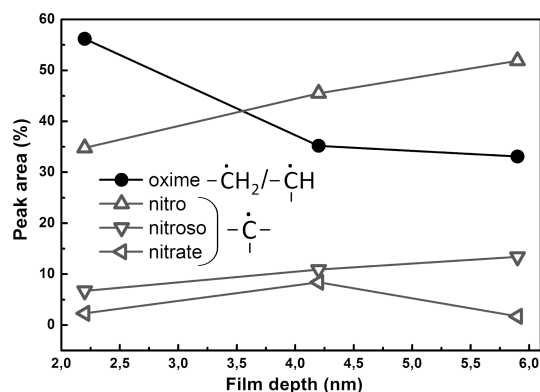


**Figure 9.** In-depth relative concentration of various nitrogen-containing groups, derived from the deconvolution of corresponding N 1s XPS spectra.

surface is subjected to interaction with plasma particles (ions, electrons) along with the plasma VUV radiation. These bombarding particles continuously break the newly formed bonds and kinetically restrict cross-linking on the top surface. Practically, all primary and secondary radicals originate from this plasma-film interphase. In contrast, the subsurface region that is shielded from interactions with plasma particles and exposed to VUV radiation for a longer duration contains much more tertiary radicals.

Preliminary grafting tests in which radicals on the surface of the PPF are expected to initiate free-radical polymerization of the monomer have been performed. The PPF with the maximum number of surface free radicals (deposited at  $P_{RF} = 200$  W) was selected for the study. 2-Ethylhexyl acrylate was chosen as a grafting agent because it contains a carboxyl functional group with a characteristic XPS peak at 289 eV, which is not present on the C1s spectrum of the PPF. C1s and O1s peaks of the nonderivatized PPF, conventionally polymerized poly ethylhexyl acrylate (as a reference) and poly(EHA) grafted PPF, i.e., after the removal of any physisorbed monomer or (nongrafted) polymer chains by selective solubilization in chloroform (see Experimental Section), are shown in Figure 10.

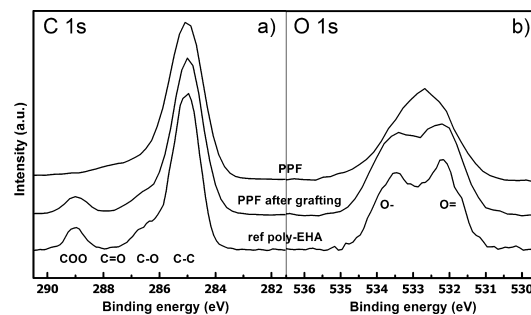


**Figure 10.** (a) C 1s XPS spectra of the PPF, poly(EHA), and grafted PPF and (b) O 1s spectra of the PPF, poly(EHA), and grafted PPF.

The comparison of C1s spectra reveals that the spectrum of the grafted polymer is very similar to the spectrum of the reference poly(EHA), exhibiting likewise the presence of COO and C–O peaks along with the main C–C peaks and the very reduced contribution of C=O peak. The appearance of the COO peak, characteristic of the poly(EHA) reference, and the almost complete disappearance of the C=O peak, indicative of

the PPF, denote the grafting of poly(EHA) chains with a thickness slightly lower than the XPS sampling depth. O1s spectra comparison yields similar results: the polymer-grafted PPF is very close in its chemical structure to poly(EHA) (O— and O= peaks) and is quite different from the PPF (single peak). These XPS findings suggest that a covalently bonded grafted layer of poly(EHA) with a thickness lower than the sampling depth of XPS (<5.9 nm) is present on the surface of the PPF. It has also been shown by the preliminary ellipsometry measurement that an increase in thickness (about 5 nm) occurs after the grafting of the poly(EHA) on the PPF. These grafting tests confirm that free radicals present on the surface of the PPF can efficiently initiate the polymerization of unsaturated monomers like acrylates.

#### 4. CONCLUSIONS

Free-radical chemistry on the surface of the isopropanol-based PPF has been studied with the help of NO chemical derivatization in combination with XPS analysis. After validation and adaptation of the derivatization method it has been found that the amount of surface free radicals increases with the deposition power up to 200 W ( $\sim 2.3 \times 10^{14}$  spin/cm<sup>2</sup>) until radical recombination presumably takes place. Growing fraction of tertiary radicals with power was attributed to the higher fragmentation of monomer in the discharge, as revealed by an in situ FTIR plasma diagnostic, and to a stronger bombardment of the growing film by ions, electrons and VUV photons. Angle-resolved XPS measurements have shown that on the top surface primary and secondary radicals are dominating, whereas there are more tertiary radicals in the subsurface region hidden from the interaction with plasma particles. Preliminary grafting tests with EHA polymerization support the possibility to covalently graft polymer chains through free-radical-induced polymerization.

#### AUTHOR INFORMATION

##### Corresponding Author

\*E-mail: rony.snyders@umons.ac.be.

##### Notes

The authors declare no competing financial interest.

#### ACKNOWLEDGMENTS

This work is supported by Belgian Government through the «Pôle d'Attraction Interuniversitaire» (PAI, P7/34, "Plasma-Surface Interaction",  $\Psi$ ).

#### ABBREVIATIONS

PPF, plasma polymer film(s)  
XPS, X-ray photoelectron spectroscopy  
FTIR, fourier transform infrared spectroscopy  
EHA, 2-ethylhexyl acrylate

#### REFERENCES

- (1) Muguruma, H.; Karube, I. *TrAC, Trends Anal. Chem.* **1999**, *18*, 62–68.
- (2) Muguruma, H. *TrAC, Trends Anal. Chem.* **2007**, *26*, 433–443.
- (3) Förch, R.; Chifén, A. N.; Bousquet, A.; Khor, H. L.; Jungblut, M.; Chu, L. Q.; Zhang, Z.; Osey-Mensah, I.; Sinner, E. K.; Knoll, W. *Chem. Vap. Deposition* **2007**, *13*, 280–294.
- (4) Hiratsuka, A.; Karube, I. *Electroanalysis* **2000**, *12*, 695–702.
- (5) Hamilton-Brown, P.; Gengenbach, T.; Griesser, H. J.; Meagher, L. *Langmuir* **2009**, *25*, 9149–9156.
- (6) Park, Z. T.; Choi, Y. S.; Kim, J. G.; Boo, J. H. *J. Mater. Sci. Lett.* **2003**, *22*, 945–947.
- (7) Yu, Y. J.; Kim, J. G.; Cho, S. H.; Boo, J. H. *Surf. Coat. Technol.* **2003**, *162*, 161–166.
- (8) Shi, F. F. *Surf. Coat. Technol.* **1996**, *82*, 1–15.
- (9) Chan, C. M.; Ko, T. M.; Hiraoka, H. *Surf. Sci. Rep.* **1996**, *24*, 1–54.
- (10) Jiang, H.; Hong, L.; Venkatasubramanian, N.; Grant, J. T.; Eyink, K.; Wiacek, K.; Fries-Carr, S.; Enlow, J.; Bunning, T. J. *Thin Solid Films* **2007**, *515*, 3513–3520.
- (11) Yasuda, H. *Plasma Polymerization*; Academic: Orlando, FL, 1985.
- (12) Smith, D. L. *Thin Film Deposition—Principles and Practice*; McGraw-Hill: New York, 1995.
- (13) Ohring, M. *Materials Science of Thin Films—Deposition and Practice*; Academic Press: San Diego, CA, 2002.
- (14) Yasuda, H.; Yasuda, T. *J. Polym. Sci., Part A: Polym. Chem.* **2000**, *38*, 943–953.
- (15) Meyer-Plath, A. *Vak. Forsch. Prax.* **2004**, *16*, 118–125.
- (16) Meyer-Plath, A. *Vak. Forsch. Prax.* **2005**, *17*, 40–46.
- (17) Holländer, A.; Wilken, R.; Behnisch, J. *Surf. Coat. Technol.* **1999**, *116–119*, 788–791.
- (18) Gengenbach, T. R.; Vasic, Z. R.; Li, S.; Chatelier, R. C.; Griesser, H. J. *Plasmas Polym.* **1997**, *2*, 91–114.
- (19) Gengenbach, T. R.; Chatelier, R. C.; Griesser, H. J. *Surf. Interface Anal.* **1996**, *24*, 271–281.
- (20) Whittle, J. D.; Short, R. D.; Douglas, C. W. I.; Davies, J. *Chem. Mater.* **2000**, *12*, 2664–2671.
- (21) Waterhouse, A.; Yin, Y.; Wise, S. G.; Bax, D. V.; McKenzie, D. R.; Bilek, M. M. M.; Weiss, A. S.; Ng, M. K. C. *Biomaterials* **2010**, *31*, 8332–8340.
- (22) Yin, Y.; Bilek, M. M. M.; McKenzie, D. R.; Nosworthy, N. J.; Kondyurin, A.; Youssef, H.; Byrom, M. J.; Yang, W. *Surf. Coat. Technol.* **2009**, *203*, 1310–1316.
- (23) Yin, Y.; Wise, S. G.; Nosworthy, N. J.; Waterhouse, A.; Bax, D. V.; Youssef, H.; Byrom, M. J.; Bilek, M. M. M.; McKenzie, D. R.; Weiss, A. S.; Ng, M. K. C. *Biomaterials* **2009**, *30*, 1675–1681.
- (24) Tan, K. L.; Woon, L. L.; Wong, H. K.; Kang, E. T.; Neoh, K. G. *Macromolecules* **1993**, *26*, 2832–2836.
- (25) Oehr, C.; Müller, M.; Elkin, B.; Hegemann, D.; Vohrer, U. *Surf. Coat. Technol.* **1999**, *116–119*, 25–35.
- (26) Wavhal, D. S.; Fisher, E. R. *Langmuir* **2003**, *19*, 79–85.
- (27) Wilken, R.; Holländer, A.; Behnisch, J. *Macromolecules* **1998**, *31*, 7613–7617.
- (28) Siow, K. S.; Britcher, L.; Kumar, S.; Griesser, H. J. *Plasma Processes Polym.* **2006**, *3*, 392–418.
- (29) Kuzuya, M.; Ito, K.; Kondo, S. I.; Yamauchi, Y. *Thin Solid Films* **1999**, *345*, 85–89.
- (30) Kuzuya, M.; Yamauchi, Y. *Thin Solid Films* **1998**, *316*, 158–164.
- (31) Wilken, R.; Holländer, A.; Behnisch, J. *Surf. Coat. Technol.* **1999**, *116–119*, 991–995.
- (32) Teng, R.; Yasuda, H. K. *Plasmas Polym.* **2002**, *7*, 57–69.
- (33) Ulbricht, M.; Belfort, G. *J. Membr. Sci.* **1996**, *111*, 193–215.
- (34) Ghasemi, M.; Minier, M.; Tatoulian, M.; Arefi-Khonsari, F. *Langmuir* **2007**, *23*, 11554–11561.
- (35) Holländer, A. *Surf. Interface Anal.* **2004**, *36*, 1023–1026.
- (36) Holländer, A.; Kröpke, S.; Pippig, F. *Surf. Interface Anal.* **2008**, *40*, 379–385.
- (37) Ivanov, V. B.; Behnisch, J.; Holländer, A.; Mehdorn, F.; Zimmermann, H. *Surf. Interface Anal.* **1996**, *24*, 257–262.
- (38) Moulder, J. F.; Stickle, W. F.; Sobol, I. P. E.; Bomben, K. *Handbook of X-ray Photoelectron Spectroscopy*, 2nd ed.; Perkin Elmer Corporation: Eden Prairie, MN, 1992.
- (39) Briggs, D.; Seah, M. P. *Practical Surface Analysis by Auger and X-ray Photoelectron Spectroscopy*; John Wiley & Sons: Chichester, U.K., 1983.
- (40) Biederman, H. *Plasma Polymer Films*; Imperial College Press: London, 2004.

(41) Friedrich, J.; Kühn, G.; Gähde, J. *Acta Polym.* **1979**, *30*, 470–477.

(42) Kuzuya, M.; Yamashiro, T.; Kondo, S. I.; Sugito, M.; Mouri, M. *Macromolecules* **1998**, *31*, 3225–3229.

(43) Mitchell, A. C. G.; Zemansky, M. W. *Resonance Radiation and Excited Atoms*; Cambridge University Press: Cambridge, U.K., 1977.